Modeling Pollutant Release from a Surface Source during Rainfall Runoff

M. Todd Walter,* J.-Y. Parlange, M. F. Walter, X. Xin, and C. A. Scott

ABSTRACT

Though runoff from manure spread fields is recognized as an important mode of nonpoint-source pollution, there are no models that mechanistically describe transport from a field-spread manure–type source. A mechanistic, physically based model for pollutant release from a surface source, such as field-spread manure, was hypothesized, laboratory tested, and field-applied. The primary objective of this study was to demonstrate the potential applicability of a mechanistic model to pollutant release from surface sources. The laboratory investigation used stable sources and a conservative "pollutant" (KCl) so that the dynamic effects of source dissolution and chemical transformations could be ignored and transport processes isolated. The field investigation used runoff and soluble reactive phosphorus (SP) data collected from a dairy-manure-spread field in the Cannonsville watershed in the Catskills region of New York State. The model predictions corroborated well with observations of runoff and pollutant delivery in both the laboratory and the field. "Pollutant" release from surface sources was generally predicted within 11% of laboratory KCl measurements and field SP observations. Laboratory flume runoff predictions with 15 and 26% errors for 25 and 15 mm h^{-1} simulated rainfall intensity experiments, respectively, represented root mean square errors of less than 0.2 mL s^{-1}. A 26% error was calculated for overland flow predictions in the field, which translated into approximately a 39 mL s^{-1} error. Results suggest that the hypothesized model satisfactorily represents the primary mechanisms in pollutant release from surface sources.

Though runoff from manure spread fields is commonly identified as an important form of nonpoint-source pollution, primarily with respect to nutrients, sediment, oxygen demanding compounds, and pathogens (Young, 1976; USEPA, 1990a,b; Kramer et al., 1995), there are no models that mechanistically describe transport from a field-spread manure–type source. The objective of this project was to create and test a simple pollutant release model that describes mechanisms for pollutant release from manure-like sources. Furthermore, in lieu of good understanding of the environmental longevity of important pollutants, particularly *Cryptosporidium parvum* (Brush, 1997), the study focus was limited to conservative pollutants. A conservative assumption provides a worst-case scenario. However, the model is not specific to any particular pollutant; in fact, different pollutants were used in the laboratory and field portions of the project.

Agricultural runoff water quality research has primarily been through field experiments (e.g., Young and Mutchler, 1976; Khaleel et al., 1980; Westerman and Overcash, 1980; Edwards and Daniel, 1993). The modeling efforts aimed at predicting pollutant release from manured fields have been, by and large, empirical and primarily focused on particulate transport (Wischmeier and Smith, 1978; Khaleel et al., 1979a,b). Wang et al. (1994, p. 123) developed a model to simulate runoff transport of land-applied manure constituents that used the convective dispersion equation and the Green and Ampt (1911) equation (Mein and Larson, 1973). While Wang et al.'s (1994, p. 123) model is largely mechanistic (Ibrahim and Scott, 1990), because it addresses sources that may not contact the ground, it simplifies the processes around the pollutant source, assuming that rainfall leaches all soluble constituents from the manure. In contrast, this project explicitly assumes an interaction between the runoff and the surface sources.

While the approach used in this project assumes nonreactive contaminants, its application is not limited to these. The theory presented here is general, applicable to other substances, and easily modified to account for important pollutant transformations. For example, phosphorus, which has received particularly acute attention in recent years, is considered in this study because it has been linked to eutrophication and associated ecosystem deterioration. Eutrophication seriously impairs the value of water bodies as recreation areas and drinking water sources (Bouldin et al., undated; Sharpley and Smith, 1992). A major source of P loading to surface waters in the northeastern United States is dairy farm manure spreading; this problem is exacerbated by a trend toward higher P levels in feed rations over the

M. Todd Walter, Environmental Science, Univ. of Alaska Southeast, Juneau, AK 99801. J.-Y. Parlange and M.F. Walter, Dep. of Agricultural and Biological Engineering, Cornell Univ., Ithaca, NY 14853-5701. X. Xin, 11459 N. 28th Drive, #1094, Phoenix, AZ 85029. C.A. Scott, IIMI, CIMMYT, Apartado #370, P.O. Box 60326, Houston, TX 77205. Received 13 Feb. 2000. *Corresponding author (mtw5@cornell.edu).

Published in J. Environ. Qual. 30:151–159 (2001).

Abbreviations: α, turbulent flow resistance parameter; A, source's horizontal cross-sectional area; c, pollutant concentration; c_0, initial pollutant concentration; D, diffusivity; h, height of overland flow; h_b, height of flow through pollutant source; H, total source height; i, rainfall intensity; J_b, solute uptake rate from bottom region of the source; K_s, saturated hydraulic conductivity; m, turbulent flow resistance parameter; M_b, cumulative mass release from bottom region; M_{ud}, cumulative diffusive mass release from upper region; M_{uc}, cumulative convective mass release from upper region; n, Manning's roughness coefficient source porosity; q, flow discharge per unit width; s, surface slope; SP, soluble reactive phosphorus; t, time; t_b, time to steady state horizontal flow through source; t_r, time to end of rain; t_s, time to steady state overland flow; u, flow velocity; v_b, volume of solution in the bottom region of the source; v_o, volume of water applied to the watershed until t_s; v'_o, back water volume; w, width of flow regime; x, distance from top of flow regime (watershed); z, vertical distance.

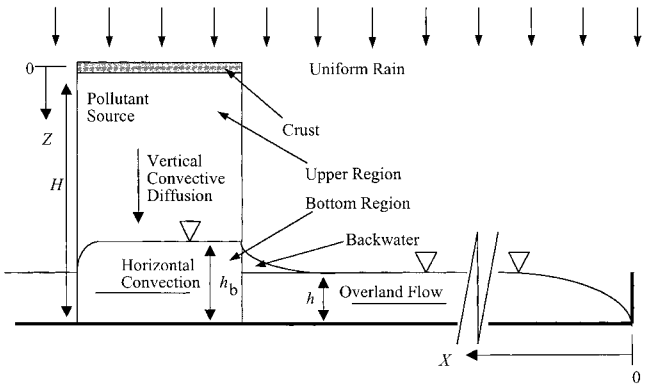

Fig. 1. Schematic of the conceptual model.

past 50 yr (Klausner and Bouldin, 1983) and increasing animal intensity (Sharpley et al., 1994). Better understanding of contaminant transport processes from surface sources, especially field-spread manure, will ultimately lead to better solutions for controlling the associated problems.

The objective of this study is to present a mechanistic mathematical model for pollutant release from a surface source and demonstrate its effectiveness in both controlled laboratory experiments and in a field application. The laboratory experiments investigate the individual modeled processes with well-defined initial and boundary conditions, thus corroborating modeled results with well-understood measurements. Because of the limitations in experimental design, the runoff portion of the model is experimentally tested independently from the pollutant release portion. Field application provides insights into the degree in which the model captures the primary processes present in the environment.

THEORY

Figure 1 diagrams the conceptual model. Pollutant release involves two processes, horizontal convection, which occurs in the bottom region of the source, and vertical convective diffusion and/or dispersion from the upper region of the source. Henceforth, parameters associated with the bottom and upper regions are designated with a subscript "b" and "u" respectively. The pollutant transport mechanisms for the bottom region and upper region of the source are modeled as independent processes. The justification for the uncoupling of these processes lies in the assumption that the time required to flush out contaminates from the lower region, t_b, is much shorter than the time required to flush out contaminates from the upper region (Xin, 1996).

The height of the boundary between the upper and bottom regions, h_b (Fig. 1), is defined by the Boussinesq (1903) equation using the Dupuit (1863) assumption and kinematic approxiation:

$$q = -h_b K_s s \qquad [1]$$

where q is the runoff discharge passing through the source ($m^2 s^{-1}$), K_s is the saturated hydraulic conductivity of the source ($m\ s^{-1}$), and s is the surface slope (negative).

The modeled source matrix is stable and static. The possibility of a crust over the source, as is occasionally observed over dairy manure, is considered in this model; like the source matrix, the crust is stable and static. At time $t = 0$, the source is essentially saturated so that there is no wetting time or change in volumetric storage within the source.

Horizontal Model (Bottom Region)

Xin (1996) showed that horizontal pollutant transport in the bottom region is dominated by convection (i.e., dispersive terms are negligible) driven by overland flow passing through the bottom of the source (Fig. 1). The expressions for overland flow, q, are derived from de-St. Venant's continuity equation (see Appendix) and can be concisely characterized by the following equations:

Henderson and Wooding (1964) $\quad q = \alpha h^m \qquad [2]$

Rising Limb of Hydrograph ($0<t<t_s$):

$$q = \alpha(it)^m \qquad [3]$$

Steady Flow portion of Hydrograph ($t_s<t<t_r$):

$$q = \alpha(it_s)^m \qquad [4a]$$

Time to steady state flow $\quad t_s = \left(\frac{x}{\alpha i^{m-1}}\right)^{\frac{1}{m}} \qquad [4b]$

Recession Limb of Hydrograph ($t_r<t$):

$$t = \frac{x - \frac{q}{i}}{\alpha^{\frac{1}{m}} m q^{\frac{m-1}{m}}} + t_r \qquad [5]$$

where i is the effective rainfall intensity ($m\ s^{-1}$), h is the depth of flow (m), t is time (s), t_s is time from the start of rainfall to reach steady flow (s), t_r is rainfall duration (s), x is the downslope distance (m), and α and m are flow resistance and flow regime parameters, respectively (see Appendix).

The differential equation describing convective transport can be expressed as:

$$\frac{\partial c}{\partial t} = -u\frac{\partial c}{\partial x} - i\frac{c}{h} + \frac{J_b}{h} \qquad [6]$$

where c is the concentration of pollutant ($mmol\ m^{-3}$), u is the convective velocity (q/h: $m\ s^{-1}$), h is the depth of flow (m), and J_b is the rate of solute uptake from the source into the flow ($mmol\ m^{-2} s^{-1}$). The bottom region is flushed of pollutant at $t = t_b$. Equation [6] can be solved for concentration, c, of solution leaving the bottom region using the relationships for h from Eq. [2], [3], and [4a]:

$$c = \frac{J_b}{i} \quad \text{for } t < t_b < t_r, \qquad [7]$$

The cumulative mass leaving from the bottom region, M_b, as a function of time is:

$$M_b = -cqwt \quad \text{for } t < t_b \qquad [8]$$

where w is the source width (m) perpendicular to flow. Any overland flow discontinuities near the source resulting from possible crusting are negligible because of the vastly larger spatial extent of a basin relative to a pollutant source. As long as no significant rainfall is stored on the crust, q is the cumulative flow over and through the source, and the concentration, then, is the flow-weighted average concentration of the contaminated through-flow and clean "over-crust" flow.

The mechanism for rate of pollutant uptake from the source into the flow, J_b, may be largely dependent on the characteristics of a particular contaminant (e.g., its dissolving, dissolution, or desorption rates) and is beyond the scope of this study. As

shown later in this paper, for some pollutants this mechanism is very rapid and its value can be estimated indirectly without full understanding of uptake mechanics. Also, the fundamental basis for the model presented here can be analytically extended to incorporate a larger range of flushing situations (i.e., it is not mathematically limited to the situation where the period of rainfall, t_r, is greater than t_b). Unfortunately, though the mathematics had been derived, laboratory limitations inhibited investigation of other scenarios.

Vertical Model (Upper Region)

Pollutant is transferred downward from the upper region to the bottom region via convective dispersion when there is significant vertical water flux and via diffusion when there is little vertical water flow through the source (e.g., when the source is crusted).

When convective dispersion is the dominant transport mechanism the simplest modeling approach is to assume that the concentration of solution released from the source follows a step function:

$$c = c_o \text{ while pollutant is available in upper region of the source}$$

$$c = 0 \text{ when all available pollutant is removed from the upper region of the source} \quad [9]$$

Thus, the cumulative mass leaving the upper region by convective dispersion, M_{uc}, is:

$$M_{uc} = cAit \quad [10]$$

where c is determined by Eq. [9] and A is the source's horizontal cross-sectional area (m^2).

When there is little or no vertical water flow through the source, diffusion dominates the vertical pollutant transport. Because diffusion requires a concentration gradient, the process is modeled by assuming no diffusive movement until the bottom region's concentration is effectively zero (i.e., $t \geq t_b$). The upper region is approximated as a semi-infinite region, bounded on the lower end by the top of the bottom region, h_b (Fig. 1), where the concentration is zero for $t \geq t_b$. Carslaw and Jaeger (1959) showed that the concentration gradient in the upper region can be written as:

$$\frac{\partial c}{\partial z} = \frac{c_o}{\sqrt{\pi D(t - t_b)}} \quad [11]$$

where c_o is the initial concentration, assumed to be initially homogenous in the upper region (mmol m^{-3}) and D is the diffusivity ($m^2\ s^{-1}$). Fick's law can be used to describe diffusive flux from the upper region, J_u:

$$J_u = -D\frac{\partial c}{\partial z} \quad [12]$$

Replacing the differential in Eq. [12] with Eq. [11] and integrating, the cumulative mass removed from the upper region by diffusion, M_{ud}, is

$$M_{ud} = 2Ac_o\sqrt{\frac{D}{\pi}}(t - t_b)^{1/2} \quad [13]$$

where A is the source's horizontal cross-sectional area (m^2), assumed constant for this study.

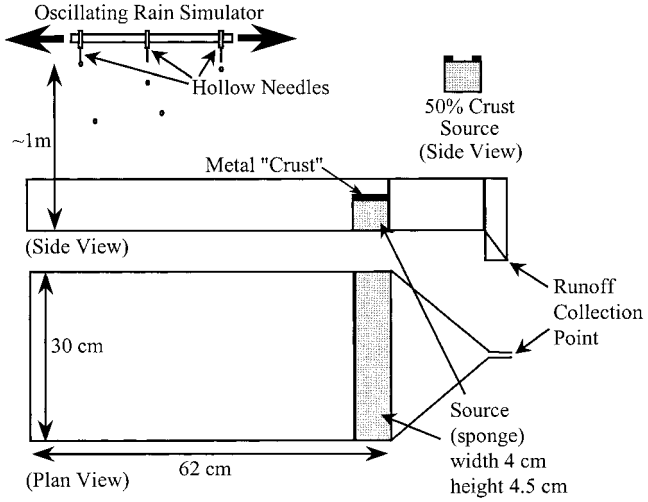

Fig. 2. Experimental flume setup. The flume is metal.

LABORATORY EXPERIMENTAL METHOD

There were two sets of laboratory experiments. The first two experimental runs tested the runoff model developed for this investigation. The second set consisted of three experimental runs that tested the pollutant release model. The runoff model was tested separately to help isolate uncertainties in the pollutant release model independently from runoff model uncertainties.

Figure 2 shows the metal flume setup used to test the models in the laboratory. The slope of the flume, s, was 0.065. Based on Baltzer and Lai (1968), Manning's n was taken as 0.05. Based on work done by Xin (1996), the source conductivity, K_s, was taken as 50 cm min^{-1}. Each experiment was 30 min long. The runoff model was tested under two rainfall intensities, 25.4 mm h^{-1} and 15.2 mm h^{-1}, with no pollutant source in the flume. The pollutant release model was tested using 24 mm h^{-1} rainfall intensity and a sponge source as described below. The rainfall simulator generated raindrops with hollow needles located ~1 m above the flume. The needles were spaced ~10 cm apart along a metal rod that oscillated laterally and longitudinally above the flume (Fig. 2); the mechanisms for the two oscillating directions were independent of each other. Water was pumped to the individual needles through plastic tubing with a peristaltic pump.

For the pollutant release experiments, three conditions were examined in the laboratory: the case with no crust on the source, the case with complete or full crusting, and an intermediate, 50% crusting, scenario. A rectangular sponge, presoaked in a solution of KCl, was used to simulate a generic conservative pollutant source. The initial concentration in the sponge was approximately 1 mmol L^{-1}; actual values ranged from 1.0 to 1.3 mmol L^{-1}. The rainwater was pretested for KCl to ensure that no additional pollutant was entering the system. Pollutant crusts were simulated using metal covers; the complete crust was a metal cover over the entire source; the 50% crust was a metal cover over half the source's top surface (Fig. 2). Diffusivity was taken as 2×10^{-5} $cm^2\ s^{-1}$ (typical for ionic solutes in water).

Effluent from the flume was collected every 10 s for the first minute, once per minute for the next 29 min, and again every 10 s for the recession period after rainfall ceased. Sampling duration was 10 s. KCl concentration was measured using a precalibrated conductivity meter; care was taken to maintain constant room temperature for all conductivity measurements to avoid errors arising from conductivity's thermal sensitivity. Due to the sponge's large pores, substantial and prolonged drainage was observed. Experimental data were adjusted using an empirical drainage curve, developed from laboratory sponge-drainage measurements, for mass removed via drainage; typically about 4 mm drained from the sponge during the experiment. Before and after the set of experiments, simulated rainfall uniformity was checked using Christian's coefficient, C_u (James, 1988, p. 453). Values for C_u were 0.90 and 0.91, indicating good uniformity.

Xin (1996) demonstrated in similar experiments that the time required to flush the bottom region of its original pollutants is short, depending primarily on the time to establish a steady bottom region. By the time steady state in the bottom region was fully established the region was essentially flushed. J_b can be approximated as the total mass of salt in the bottom region per unit area divided by the time to establish steady flow in the bottom region. It follows then that t_b, the time to flush pollutants from the bottom region, can be estimated as the time to establish steady flow in the bottom region:

$$t_b = \frac{v_b + v_o + v_o'}{iLw} \quad [14]$$

where v_b (m^3) is the volume of solution in the bottom region of the source, v_o (m^3) is the cumulative volume of water applied to the flume–watershed between $t = 0$ and $t = t_s$, and v_o' (m^3) is the backwater volume. Approximating q as iLw, combining Eq. [2] and [4b] for h, multiplying by the flume's width, w (m), and integrating over the flume's length, L (m), v_o is:

$$v_o = wLi[t_s(L)] \quad [15]$$

where the function $t_s(L)$ is the time to steady overland flow at $x = L$. The flume's simple geometry yields the following expression for v_b:

$$v_b = \frac{h_b}{H} v_t \quad [16]$$

where H is the total source height (m), h_b is the depth of water flowing through the source (m) (Eq. [1]) (Fig. 1), and v_t is the total solution volume in the source (m^3); measured values ranged from 300 to 450 mL depending on drainage. The backwater volume, assumed to be greater than v_o, is estimated assuming simple level-pool damming of runoff water behind the source:

$$v_o' = w\frac{[h_b - h(t_s)]^2}{2s} \quad [17]$$

By the definition discussed earlier, the mass transfer flux for the bottom region is:

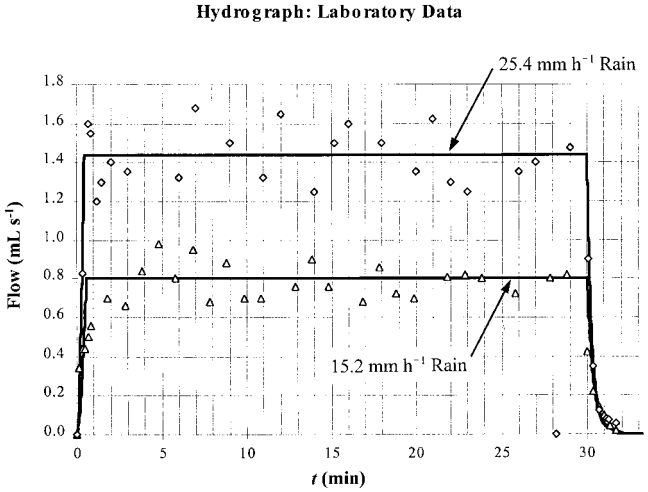

Fig. 3. Kinematic model experiment at two rainfall intensities (laboratory results). Calculated steady state flow depths were 1.8 and 2.5 mm for the 15.2 mm h^{-1} and 25.4 mm h^{-1} rain intensities, respectively. Triangles and diamonds = observed data.

$$J_b = \frac{v_b c_o}{At_b} \quad [18]$$

LABORATORY RESULTS

Figures 3 and 4 show the agreement between the kinematic model for runoff in the flume and experimental data. A statistical comparison between predicted and observed values is shown in Table 1. The experiment represented in Fig. 4 involved a *sponge dam* for which this kinematic model does not explicitly account.

Figure 5 and Table 2 show the agreement between the modeled and observed cumulative pollutant release results for the three experiments.

There was experimental variation in the initial KCl concentration and the initial solution volume in the sponge, ±0.05 mmol mL^{-1} (approx. 5%) and ±75 mL (20%), respectively. Therefore, to eliminate these

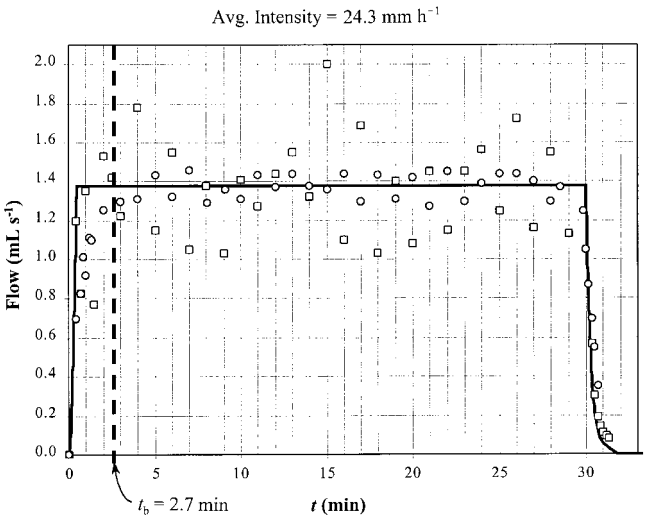

Fig. 4. Kinematic model results from the no-crust and 50%-crust experimental runs. Calculated steady state flow depth was 2.4 mm. Laboratory data: squares = no crust, circles = 50% crust.

Table 1. Statistical results for kinematic flow laboratory experiments.

	Predicted vs. observed		
	(Fig. 3) High intensity 25.4 mm h^{-1}	(Fig. 3) Low intensity 15.2 mm h^{-1}	(Fig. 4) Crust experiments 24.3 mm h^{-1}
N†	30	36	83
R^2	0.95	0.86	0.79
Standard error (mL s^{-1})	0.13	0.12	0.20
Mean of absolute error (mL s^{-1})	0.11	0.11	0.15
Standard deviation of absolute error (mL s^{-1})	0.10	0.10	0.14
RMSE‡ (mL s^{-1})	0.17	0.15	0.21
Relative difference§ (%)	15	26	19

† Number of observations.

‡ Root mean square error: RMSE $= \sqrt{\frac{\Sigma(\text{Obs.} - \text{Pred.})^2}{N}}$

§ Relative difference = RMSE/Mean(Obs.)

sources of variation cumulative export results are shown in terms of percent of total pollutant released.

FIELD METHODS

Field observations, at an operating dairy farm, were made on a manure-spread field in Delaware County, part of the Catskills region of New York State (Fig. 6). The field was fallow with corn (*Zea mays* L.) stalks and residue. The soil was primarily Channery silt loam. Rainfall, runoff, and phosphorus concentration data were collected from the field for the 19 and 20 June 1996 rainfall event (natural). Rainfall was measured with a tipping bucket rain gauge. Runoff was measured using a partial flume in a diversion at the low end of the field. The diversion collected both tile flow and overland runoff. Tile flow was measured directly at tile outlets using small flumes and runoff was determined via subtraction of the tile flow from the total. The flows were similarly sampled separately and, again, the runoff fraction was determined by subtraction. Both phosphorus sampling and flow measuring were automated; phosphorus samples were taken hourly by an ISCO (Lincoln, NE) automatic sampler and runoff discharge measurements were made every 15 min. The samples were tested in the laboratory for SP. Water samples were filtered through 0.45-μm filters under a vacuum of 70 kPa or less to separate the SP fraction. Soluble reactive P concentration of the filtrate was determined by measuring ascorbic acid–reduced phosphomolybdate using a Turner Instruments (Mountain View, CA) 690 spectrophotometer at 880 nm following Standard Method 424F (American Public Health Association, 1985). Note that sediment loss was negligible for this event making it ideal for this study. Also, though there was undoubtedly some SP contribution from the soil, recent research shows that it will typically account for less than 1% for this scenario (Walter et al., 2001) and was therefore not accounted for in the model investigation.

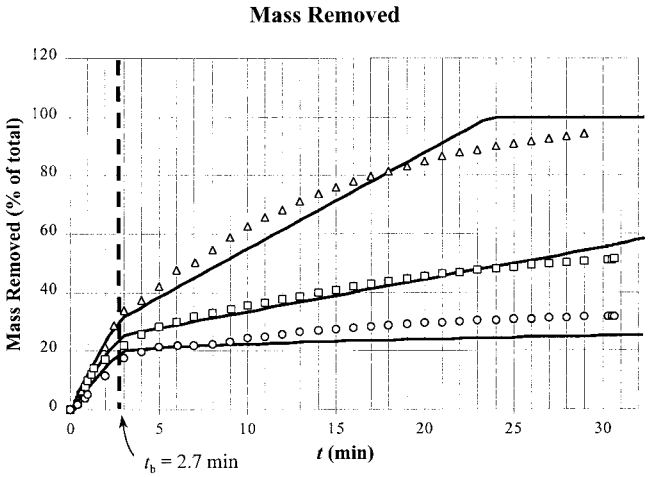

Fig. 5. Pollutant transport results, data, and model (laboratory results). Triangles = observed data for no-crust experiment; squares = observed data for 50%-crust experiment; circles = observed data for complete-crust experiment; lines = respective model predictions.

Table 2. Statistical results for cumulative pollutant release laboratory experiments.

	Predicted vs. observed		
	No crust	50% crust	Full crust
N	32	35	35
R^2	0.97	0.98	0.94
Mean (mmol)	237	141	96.1
Standard error (mmol)	19.4	8.32	9.16
Mean of absolute error (mmol)	18.5	6.96	28.8
Standard deviation of absolute error (mmol)	10.6	4.86	31.1
RMSE (mmol)	18.8	7.93	38.4
Relative difference (%)	7.9	5.6	39.9

Field parameterization for the model was difficult due to physical nonhomogeneity and multiple measurements that were unavailable (e.g., concentration of SP in prespread manure). Therefore, order of magnitude estimates and system simplifications were used to apply the model. This is consistent with the objectives of this portion of the study, namely to demonstrate model application to a field situation and determine if the model

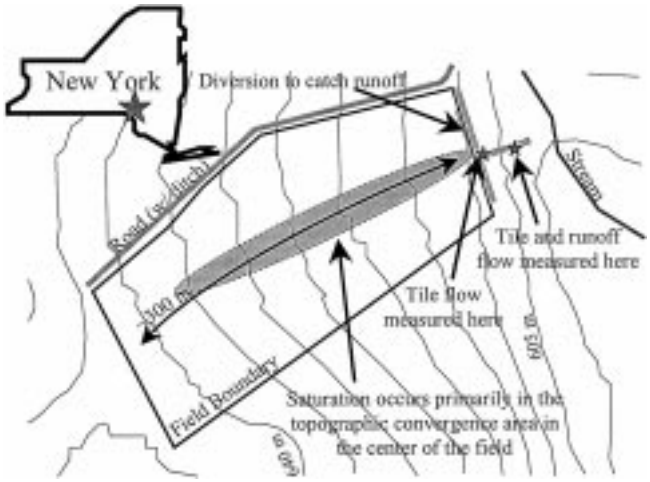

Fig. 6. Field layout.

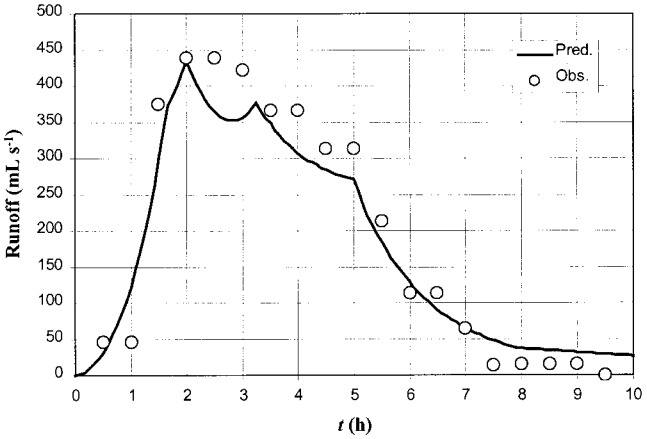

Fig. 7. Kinematic runoff model results and field data (field results): circles = observations, line = model predictions.

captures the primary mechanisms; it was not to quantify predictions with great precision. Flags were manually placed around the saturated field area (i.e., the runoff contributing area); pacing distances to approximate area showed that this area varied throughout the first few hours of the runoff event from roughly 0.2 to 0.5 ha. To incorporate this variable source area observation into the model, the width of the flow region was assumed to increase linearly over the first 3 h of the storm (this time resulted in the best fit for the hydrograph) and no infiltration was assumed to occur on the saturated areas. For simplicity, the contributing area was considered rectangular. The longest flow-path length and average slope were 300 m and 11%, respectively (Fig. 6). Though the rainfall persisted for many hours, the period modeled corresponds to the period of observed runoff; rainfall preceding runoff saturated the part of the field upon which runoff was generated. Though rainfall was measured continuously, rainfall used in the model was partitioned into two periods based on average intensities; a 2-h period of 0.4 mm h^{-1} and a 4-h period of 0.2 mm h^{-1}. The duration of these periods was dictated by the kinematic model; finer divisions of runoff would require using a kinematic model with $t_r < t_s$, which is beyond the scope of this paper. Dairy manure (with bedding) was spread (17.8 Mg ha^{-1}) simultaneously with the rainfall so source crusting was assumed negligible.

The mathematical development used for the laboratory experiments was directly applied to the field with the elimination of backwater accumulation because overland flow is free to flow around manure clumps. No modifications were made for preferential flow around sources. Based on qualitative visual observations, the source was assumed to be well distributed across the lower portion of the contributing area in saturated clumps approximately 2.5 cm high, which occupied roughly 40% of the total runoff-contributing area. Manure conductivity of 50 cm min^{-1} was used. The concentration of SP in the manure, c_0, was approximated by using the highest observed concentration (4 mg L^{-1}). The authors recognize that the choice of phosphorus was potentially non-ideal because of its strong soil sorption–desorption mechanisms, but used it anyway because of data availability.

Table 3. Statistical analysis of field results.

	Predicted vs. observed	
	Overland flow	Cumulative phosphorus release
	mL s^{-1}	mg†
N	19	10
R^2	0.93	0.99
Mean	205	2920
Standard error	39	675
Mean of absolute error	19	718
Standard deviation of absolute error	33	724
RMSE	53	940
Relative difference (%)	26	7

† Sample mean.

FIELD RESULTS

The field results are summarized in Fig. 6 and 7 and statistical comparisons are shown in Table 3. Figure 7 shows the agreement between the kinematic model and observed flow; note the time to establish the saturated runoff contributing area was adjusted to provide the best visual fit of the model to the data. A good fit in the runoff model was needed to meaningfully identify possible missing mechanisms in the pollutant release model. Figure 8 shows observed and predicted cumulative pollutant release.

DISCUSSION

The kinematic flow equations corroborated well with the measured data. The oscillating nature of the lab data, seen in Fig. 3 and 4, can be largely attributed to the rainfall simulator's oscillating mechanism, traveling up and down the flume. The no-crust experiment, which shows the most obvious flow oscillations (squares in Fig. 4), was run immediately before the 50%-crust experiment, which shows much less dramatic oscillatory characteristics (circles in Fig. 4). These differences are perhaps explained by differences in air entrapment within the rainfall simulator's tubing or by fortuitous measurement timing in the second experiment. It is probable,

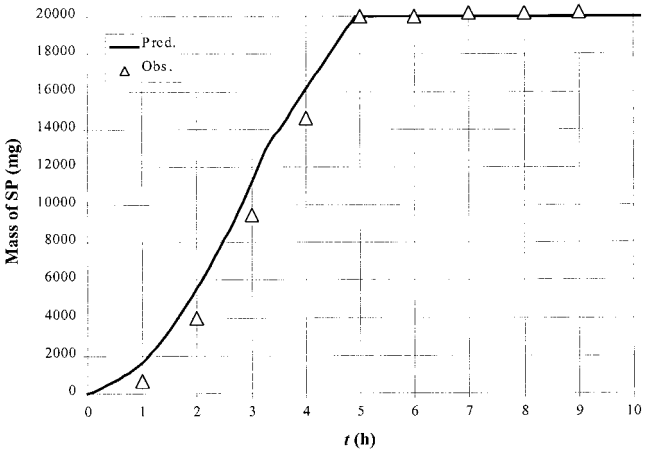

Fig. 8. Pollutant transport model vs. pollutant delivery from the field (field results). Triangles = observations, line = model predictions. SP = soluble reactive phosphorus.

anyway, that much of the observed flow variability is inherent to the experimental apparatus, especially the rain simulator, which is oscillatory in nature.

In Fig. 4, the attenuation of the rising hydrograph limb, especially for the 50%-crust data (circles), shows the *damming* effect of the sponge and agrees well with t_b; that is, the data reach the steady state model at t_b (2.67 min). Note that the purpose of the runoff model is to determine the flow reaching the source so this damming does not affect the overall model (i.e., how runoff and pollutant sources interact). If a method had been conceived to measure the runoff immediately upslope of the sponge (pollutant source), the results would most likely have looked very much like those in Fig. 3. The strong correlation between observed and modeled pollutant releases does not warrant a more rigorous approach to modeling runoff.

The end of the early steep, linear section of the cumulative pollutant release curves in Fig. 5 are at $t = t_b$, estimated with Eq. 14 through 17. Though h, h_b, and v_o' were not directly measured, the good agreement between the data and the calculated t_b (Fig. 4 and 5) suggest that the approximations used are adequate for this experiment.

The field runoff data agreed well with the kinematic equation (Fig. 7 and Table 3), indicating that this methodology has good potential for simulating runoff hydrographs for variable source areas. It also suggests that infiltration into the saturated regions is indeed negligible, as assumed. A smoother-modeled hydrograph is attainable with smaller storm periods but, as discussed earlier, this approach was beyond the scope of this paper. Further investigation is needed to generalize the model to other field conditions.

As indicated in Tables 2 and 3, the pollutant transport model corroborates well with the general observed trends in both field and laboratory observations. The field results show particularly good agreement in that they were much better than anticipated. The early ($t < t_b$), linear portions of the lab curves show good agreement and suggest that the highly simplified nature of Eq. [18] is adequate within the boundaries and precision of these experiments.

The full-crust lab experiment showed the worst statistical agreement between measurements and predictions. While the full-crust experiment corroborated well with predictions during the initial flushing stage, the total cumulative mass release prediction was about 20% lower than observed. The discrepancy in total cumulative pollutant release is due to an underprediction of the delayed, vertical flux, stage of release. During this period, the model underpredicted by approximately 30%. This suggests that diffusion is not the only vertical transport mechanism or that the diffusion coefficient was too low for the very concentrated solution used in these experiments. One possible explanation is the presence of vertical convection via rainwater entering the upstream face of the sponge, which was unprotected (uncrusted). Assuming the exposed upstream face corresponds to a 10% uncrusted area of the source, and that convected pollutant from this area can be added to the diffused-out pollutant, corroboration of predicted pollutant release by measurements improves; R^2 is 0.98 and relative difference is 4.8%. Though the effects of increased solute concentration on the diffusion coefficient were not investigated, increasing the diffusion coefficient fourfold makes the prediction–observation agreement similar to the other two lab experiments (i.e., R^2 is 0.98 and relative difference is 5.3%). Xin (1996) suggested a dispersion mechanism along the boundary between the upper and bottom regions to explain the greater-than-diffusion-alone pollutant release. This explanation may justify a higher "effective" diffusion coefficient.

In the 0- and 50%-crust lab cases the model's rate of mass removal for $t > t_b$ is much more linear than the observations (Fig. 5). This suggests a missing or inadequately described mechanism in the model that is present in *sponge* leaching. One possible explanation is that this model is missing a dispersion mechanism that would presumably add curvilinear characteristics to the predictions. However, the strong statistical agreement between observed data and predicted results (Tables 1 and 2) with the current simplified model did not warrant additional complication for this study.

As previously stated, the field results for this study showed very good agreement between the model and observations, probably better than most other nonpoint-source models and certainly better than the authors expected given the crude model parameterization. A sensitivity analysis was performed on some of the parameters; individual parameters were independently adjusted by ±10% and the associated changes in the predicted results investigated. The height of the source, H, the field slope, s, Manning's n, and the width of the saturated area had no discernable affect on the results at the level of statistical precision in Table 3. Table 4 shows the sensitivity statistics for the field results associated with maximum extent of saturated area, distribution of pollutant, and length of saturated area, L. Comparing Tables 3 and 4, the model is not overly sensitive to any one parameter. Note that some permutations appear to actually improve the model performance, demonstrating that the original parameters were uncalibrated.

Upon close inspection of the modeled field results,

Table 4. Sensitivity of selected field parameters.

	Distribution of pollutant sources		Saturated area		Length of saturated area, L	
	+10%	−10%	+10%	−10%	+10%	−10%
R^2	0.99	0.99	1.00	0.99	0.96	0.99
Standard error (mg)	646	647	527	790	1636	879
RMSE (mg)	940	940	1838	1656	1800	909
Relative difference (%)	7	7	12	12	13	6

less than 0.5% (0.45%) of the total pollutant release was from the direct flushing due to runoff passing through the sources. Therefore, almost all of the pollutant (SP) came from vertical advective dispersion. This adds credence to the assumption used in the Wang et al. (1994, p. 123) model, that all pollutant is vertically leached from the source. It also implies that source crusting could potentially have a significant effect on pollutant release. This result also suggests that our model is insensitive to source conductivity for this scenario; in fact, order of magnitude changes in source conductivity had little effect on these results. These results make incorporating a more complicated runoff model to account for preferential flow around isolated sources unjustifiable. It is also important to note that these results are from one relatively prolonged, low-intensity storm and should not be overly generalized. For shorter storms, the durations of horizontal flushing and vertical leaching would be more similar and the magnitudes from each less disparate. It is interesting to note that without the physical basis of this model, the observations in the above paragraph would not be possible.

This study shows drastic pollutant release restriction potential for crusted pollutant sources such as field-spread dairy manure. As shown in Fig. 5, the crusted source released only 25 to 30% as much pollutant at the fully uncrusted source. For the lab conditions used, increase in pollutant release was roughly linear with degree of uncrusted area. As mentioned in the previous paragraph, the vertically leached component dominated pollutant release in our field data, suggesting even larger potential effects from source crusting.

CONCLUSION

A simple, mechanistic model was developed to represent pollutant release from surface sources. Good corroboration of the model results with both field and laboratory observations suggests that the model theory correctly accounts for the primary mechanisms of pollutant transport from field-spread manure–type pollutant sources, including potentially crusted sources. The primary strength of the model is its physical basis, making it adaptable to a variety of conditions, including situations where runoff flushing may dominate, as in the laboratory experiments, and situations were rainfall leaching dominate, as in the field investigation. Another strength of the model is its relative simplicity. The approximations used are obvious and easily modified to account for more complicated processes; for example, dispersive vertical flushing can be inserted in place of the current plug-flow-type mechanisms used in this study.

Work is needed to accurately parameterize field information for the model and to expand on model corroboration. Also, further thought should be given to developing methods to test extended derivations of the model shown here to account for other situations, for example, where the pollutant in the bottom region does not flush out quickly or the rainfall ends before steady state flow is established. Though further field testing is needed, the results shown above suggest potential for adaptation of this kind of mechanistic approach to farm management research and other field situations.

APPENDIX

Derivation of Overland Flow Equations

Overland flow is modeled with de-St. Venant's continuity equation:

$$\frac{\partial h}{\partial t} + \frac{\partial q}{\partial x} = i \qquad [A1]$$

where h is the depth of flow (m), q is the discharge per width ($m^2\ s^{-1}$), i is the effective rainfall intensity ($m\ s^{-1}$), t is time (s), and x is downhill distance (m). The kinematic assumption applied to the momentum equation yields (Henderson and Wooding, 1964):

$$q = \alpha h^m \qquad [A2]$$

where α and m are flow resistance and flow regime parameters respectively. For turbulent flow these parameters can be approximated with:

$$\alpha = \frac{\sqrt{s}}{n}; m = \frac{5}{3} \qquad [A3]$$

where n is the Manning roughness factor (unitless) and s is the surface slope ($m\ m^{-1}$).

The following derivation assumes constant effective rainfall rate, i. This assumption should not limit the utility of this model, as a temporally varying rainfall can be divided into small time increments and a composite hydrograph created via superposition. Using the method of characteristics, the time from the start of rainfall to reach steady flow, t_s, at any point x is:

$$t_s = \left(\frac{x}{\alpha i^{m-1}}\right)^{\frac{1}{m}} \qquad [A4]$$

Assuming the time at which the rainfall ends, t_r, is greater than t_s, and using the method of characteristics and Eq. [A1] and [A2], the flow at any point, x, can be described by Eq. [A5] through [A7]:

Rising limb of hydrograph ($0 < t < t_s$):

$$q = \alpha(it)^m \qquad [A5]$$

Steady flow portion of hydrograph ($t_s < t < t_r$):

$$q = \alpha(it_s)^m \qquad [A6]$$

Recession limb of hydrograph ($t_r < t$):

$$t = \frac{x - \frac{q}{i}}{\alpha^{\frac{1}{m}} m q^{\frac{m-1}{m}}} + t_r \qquad [A7]$$

The partial equilibrium situation, $t_r < t_s$, can be analytically described, yielding different expressions for Eq. [A6] and [A7], but is not presented here because the laboratory restrictions prevented an experimental design to allow for this situation to be adequately evaluated.

REFERENCES

American Public Health Association. 1985. Standard methods for examination of wastewater. 16th ed. Am. Water Works Assoc. and APHA, Washington, DC.

Baltzer, R.A., and C. Lai. 1968. Computer simulation of unsteady flow in waterways. J. Hydraul. Div. ASCE. 94:1083–1117.

Bouldin, D.R., H.R. Capener, G.L. Casler, A.E. Durfee, R.C. Loehr, R.T. Oglesby, and R.J. Young. Undated. Lakes and phosphorous inputs: A focus on management. Plant Sci. Info. Bull. 127. Cornell Univ., Ithaca, NY.

Boussinesq, J. 1903. Sur un mode simple d'ecoulement des nappes d'eau d'infiltration a lit horizontal avec rebord vertical tout autour lorqu'une partie de ce rebord est enlevee depuis la surface jusqu'au fond. C.R. Acad. Sci. 137:5–11.

Brush, C.F. 1997. Surface and transport properties of *Cryptosporidium parvum* oocysts. Ph.D. thesis. Cornell Univ., Ithaca, NY.

Carslaw, H.S., and J.C. Jaeger. 1959. Conduction of heat in solids. 2nd ed. Oxford Univ. Press, London.

Dupuit, J. 1863. Estudes thèoriques et pratiques sure le mouvement des eaux dans les canaux dècouverts et à travers les terrains permèables. 2nd ed. Dunod, Paris.

Edwards, D.R., and T.C. Daniel. 1993. Effects of poultry litter application rate and rainfall intensity on quality of runoff from fescuegrass plots. J. Environ. Qual. 22:361–365.

Green, W.H., and G. Ampt. 1911. Studies of soil physics, Part I: The flow of air and water through soils. J. Agric. Sci. 4:1–24.

Henderson, F.M., and R.A. Wooding. 1964. Overland flow and groundwater flow from a steady rainfall of finite duration. J. Geophys. Res. 69(8):1531–1540.

Ibrahim, B.A., and H.D. Scott. 1990. Fate of nitrogen from the disposal of poultry litter: A simulation approach. Publ. no. 148. Arkansas Water Resour. Center, Univ. of Arkansas, Fayetteville.

James, L.G. 1988. Principles of on farm irrigation system design. John Wiley & Sons, New York.

Khaleel, R., G.R. Foster, K.R. Reddy, M.R. Overcash, and P.W. Westerman. 1979a. A non-point source model for land areas receiving animal waste: III. A conceptual model for sediment and manure transport. Trans. ASAE. 22:1353–1361.

Khaleel, R., G.R. Foster, K.R. Reddy, M.R. Overcash, and P.W. Westerman. 1979b. A non-point source model for land areas receiving animal waste: IV. Model inputs and verification for sediment and manure transport. Trans. ASAE. 22:1362–1368.

Khaleel, R., K.R. Reddy, and M.R. Overcash. 1980. Transport of potential pollutants in runoff water from areas receiving animal wastes: A review. Water Res. 14:421–436.

Klausner, S., and D. Bouldin. 1983. Managing animal manure as a resource. Part II: Field management. Coop. Ext. Cornell Univ., Ithaca, NY.

Kramer, M.H., B.C. Herwaldt, G.F. Craun, R.L. Calderon, and D.D. Juranek. 1995. Waterborne disease: 1993 and 1994. J. Am. Water Works Assoc. 88:66–80.

Mein, R.G., and C.L. Larson. 1973. Modeling infiltration during a steady rain. Water Resour. Res. 9:384–394.

Sharpley, A.N., S.C. Chapara, R. Wedepohl, J.T. Sims, T.C. Daniel, and K.R. Reddy. 1994. Managing agricultural phophorus for protectin of surface waters: Issues and options. J. Environ. Qual. 23:437–451.

Sharpley, A.N., and S.J. Smith. 1992. Prediction of bioavailable phosphorus loss in agricultural runoff. J. Environ. Qual. 21:32–37.

USEPA. 1990a. Cryptosporidium workshop: Summary of a workshop held February 20, 1990 in Washington, DC. Office of Drinking Water, USEPA, Washington, DC.

USEPA. 1990b. National water quality inventory. 1988 Rep. to Congress. Office of Water, U.S. Gov. Print. Office, Washington, DC.

Walter, M.T., E.S. Brooks, J. Boll, M.F. Walter, C.A. Scott, and T.S. Steenhuis. 2001. Soluble phosphorus transport from manure-applied fields under various spreading strategies. J. Soil Water Conserv. (in press).

Wang, Y., D.R. Edwards, T.C. Daniel, and H.D. Scott. 1994. Simulation of runoff transport of animal waste constituents. ASAE, St. Joseph, MI.

Westerman, P.W., and M.R. Overcash. 1980. Short-term attenuation of runoff pollution potential or land-applied swine and poultry manure. p. 289–292. *In* Livestock waste: A renewable resource. Proc. 4th Int. Symp. on Livestock Wastes, Amarillo, TX. 15–17 Apr. 1980. ASAE, St. Joseph, MI.

Wischmeier, W.H., and D.D. Smith. 1978. Predicting rainfall erosion losses. Agric. Handb. 537. USDA-Science and Education Administration. U.S. Gov. Print. Office, Washington, DC.

Xin, X. 1996. Mathematical description of entrainment and transport of soluble pollutants in manure. M.Sc. thesis. Cornell Univ., Ithaca, NY.

Young, R.A. 1976. Effect of winter applied manure on runoff erosion and nutrient movement. ASAE Paper 76-2080. ASAE, St. Joseph, MI.

Young, R.A., and C.K. Mutchler. 1976. Pollution potential of manure spread on frozen ground. J. Environ. Qual. 5:174–179.